Utility and limitations of GPS-Interferometric Reflectometry in vegetation sensing

Clara C. Chew[a], Eric E. Small[b], Kristine M. Larson[c], Valery U. Zavorotny[d]

[a] Department of Geological Sciences, University of Colorado at Boulder

2200 Colorado Avenue, Boulder, Colorado, USA 80309

claracchew@gmail.com 1.317.281.0605

Corresponding author

[b] Department of Geological Sciences, University of Colorado at Boulder

2200 Colorado Avenue, Boulder, Colorado, USA 80309

eric.small@colorado.edu

[c] Department of Aerospace Engineering Sciences, University of Colorado at Boulder

429 UCB University of Colorado Boulder 80309

Kristinem.larson@gmail.com

[d] NOAA/Earth System Research Laboratory

325 Broadway, Boulder, Colorado, USA 80305

valery.zavorotny@noaa.gov

Keywords: radar, remote sensing, vegetation, global positioning system, reflectometry, soil

Abstract

The utility of bistatic radar remote sensing using GPS signals to estimate changes in vegetation surrounding a ground-based antenna is evaluated. A one-dimensional, plane-stratified model that simulates the response of GPS SNR data to changes in both soil moisture and vegetation is presented. The model is validated against observations of SNR data from four field sites with varying vegetation cover. The model is used to assess the ability of SNR metrics (phase and amplitude of SNR oscillations, and effective reflector height) to quantify changes in vegetation extent, specifically vegetation wet weight. This analysis shows that the amplitude of SNR oscillations may be used to estimate vegetation change when vegetation wet weight does not exceed 1 kg m^{-2}. Error introduced by the effect of soil moisture on amplitude is approximately 0.1-0.2 kg m^{-2}. When vegetation cover exceeds 1 kg m^{-2}, as it would in agricultural settings, amplitude alone cannot be used to estimate vegetation. Phase of SNR oscillations also varies consistently with vegetation up to 1 kg m^{-2}. However, phase is also very sensitive to soil moisture variations, thus limiting its ability to also measure vegetation. Effective reflector height is not a consistent indicator of vegetation change for most canopies. Beyond 1 kg m^{-2}, the constant frequency assumption used to characterize SNR fluctuations does not adequately describe observed data, most likely due to reflections from the vegetation canopy. A more complex approach to describing SNR data than the metrics used here is required to extend GPS-IR sensing to thicker canopies.

1. Introduction

Quantifying key vegetation parameters, including the timing and duration of green-up, maturity, senescence, and dormancy, is important for phenologists, climate scientists, and agriculturalists [1]. These parameters are essential in understanding the effect of shifting precipitation regimes on ecology, ensuring future food security, and in the implementation of variable-rate technologies such as fertilizer applications [2][3]. In addition, quantifying vegetation extent, such as vegetation water content, is important to soil scientists interested in using remote sensing data products for soil moisture estimation. This is because soil moisture retrievals are affected by changes in vegetation cover [4][5]. As vegetation grows, the reliability of the retrievals decreases.

Different remote sensing techniques have been developed to estimate vegetation biophysical parameters, using a variety of antennas and frequency bands. Here, we focus on microwave frequencies, which are not affected by cloud cover or available sunlight. Microwave remote sensing can be divided into two categories: passive or active. Both categories measure how microwaves are attenuated or changed by the ground surface's permittivity or dielectric constant, which is primarily a function of its water content [6]. Passive microwave remote sensing uses one receiving antenna that collects naturally-emitting microwave radiation from the ground and relates this information to changes in soil moisture or vegetation water content. Active microwave sensing uses one antenna that transmits microwaves towards the ground surface and measures their interaction with the surface. If the receiving antenna is the same as the transmitting antenna (monostatic, or one antenna), vegetation water content is related to the amount of backscatter that is received, with higher backscatter values being associated with higher water contents [7]. If the receiving antenna is different from the

transmitting antenna (bistatic, or two antennas), vegetation water content is related to the amount of forward scattering, or the amount of received power at the antenna. In this case, lower received power is correlated with higher water contents [8]. The technique described in this paper uses a bistatic antenna system.

The constellation of GPS satellites (transmitting antennas) together with ground-, plane-, or space-based receiving antennas can be used to sense environmental variables in a bistatic radar approach. Numerous investigators have employed this general technique to study the ocean and land surface [9]. Ocean studies have focused on surface height and wind speed retrieval, and both theoretical [10] and experimental studies [11] have proven the utility of the approach, even for receiving antennas that are stationed in low earth orbit [12]. Terrestrial properties may also be estimated using bistatic sensing of reflected GPS signals (e.g. [13] and [14]). However, this line of research is just beginning. A subset of these studies has been focused on vegetation. Most of these studies have used antennas or receivers specifically designed for the task [15][16]. [17] suggested that geodetic-quality antennas/receivers could be used for vegetation sensing. This technique, known as GPS-Interferometric Reflectometry (GPS-IR), is attractive because ground-based GPS networks already exist that can provide data for vegetation studies.

GPS-IR is a technique that relates changes in ground-reflected, or multipath, GPS signals (Fig. 1) to changes in environmental parameters for an area of approximately 1000 m^2 surrounding a GPS antenna. The exact sensing area depends on the number of satellite tracks used and the height of the antenna. For a single satellite track, the sensing area can be approximated using equations found in [18].

The interaction between the direct and multipath signal are recorded by GPS receivers in signal-to-noise ratio (SNR) interferograms, examples of which are shown in Fig. 2a. Several metrics can be calculated from the SNR interferogram (details in Section 2). Phase and amplitude of the interferogram have been estimated using a constant frequency model, which is based on the assumption that the soil surface is the dominant reflector [19] [20]. Alternatively, a change in the height of the primary reflector can be estimated from the SNR data and correlated with changes in snow depth and near-surface soil moisture [20][21]. However, vegetation also affects GPS multipath, which may obfuscate the soil moisture signal. Because GPS-IR uses the same microwave frequency band (L-band, ~1.2 GHz) as other remote sensing satellites, like SMOS or SMAP, this technique could be used to validate satellite soil moisture retrievals, but only if the effect of vegetation on GPS-IR is first quantified. It could also provide estimates of vegetation extent on the field scale, which is the scale most useful for agriculturalists and is intermediate to the scales of *in situ* measurements and satellite retrievals.

[17] showed that the amplitude of SNR oscillations decreases when vegetation extent is high but did not quantify this effect. A time series of SNR amplitude in Fig. 3 illustrates that this metric changes throughout the vegetation growing season. We will also show that SNR phase and effective reflector height change during the year in response to vegetation. However, the exact relationship between SNR metrics and vegetation is difficult to determine from field data alone, given the heterogeneity of field sites, the inability to perfectly characterize vegetation parameters through field sampling, noise in the observations, and the concurrent influence of soil moisture on SNR metrics.

Here, we use field data and an electrodynamic forward model developed in [22] to quantify how changes in vegetation affect SNR metrics. This model was used in [21] to illustrate the effect of changes in soil moisture on SNR metrics for a bare soil. In this study, we adapt the model by adding a layer of homogeneous vegetation on top of the soil. We also examine how vertical variations in the vegetation canopy affect metrics. First, we describe our model and validate it against field observations. The purpose of model validation is to see if we can successfully simulate the shape of the SNR curve and how SNR metrics vary with vegetation extent. Due to inherent errors in field measurements and other complexities described above, we do not expect our model to perfectly mimic field observations. Next, we use the model to quantify how SNR metrics should theoretically respond to changes in vegetation characteristics, specifically changes in vegetation wet weight, which is the amount of vegetation covering the ground in [kg m^{-2}]. Lastly, we explore when and why our metrics either succeed or fail in describing changes in vegetation state. This final analysis is important in order to conclude whether upper or lower limits of vegetation sensing are due to the SNR data themselves or shortcomings of the metrics used to describe the data.

2. GPS-IR Background

GPS-IR utilizes GPS antennas and receivers that are normally used for tectonic applications to retrieve information about changes in the environment surrounding the antenna. This technique is different from other bistatic reflectometry methods in that it does not require a specially-designed antenna or receiver in order to estimate environmental parameters (e.g. [23] and [16]). This technique is currently used at many of the already-existing

GPS stations that comprise NSF's Plate Boundary Observatory (PBO) network to estimate changes in snow depth [24].

GPS-IR takes advantage of the interference of the coherent direct and reflected GPS signals, which is recorded in SNR interferograms. This interference is greatest at grazing to low satellite elevation angles (90 degrees being defined as zenith), as shown in Fig. 2a. For environmental sensing, the SNR data are converted to a linear scale and detrended with a low-order polynomial to remove the effect of the direct signal [18]. The detrended portion, which oscillates around zero, is shown in Fig. 2b. In this paper, we will use the term SNR to mean the detrended portion of the signal.

Detrended SNR data have previously been modeled using the following equation [25]:

$$SNR = A\cos\left(\frac{4\pi H_0}{\lambda}\sin E + \varphi\right) \qquad (1)$$

H_0 is the height of the antenna, E is the elevation angle of the satellite, A is a constant amplitude, λ is the GPS wavelength, and φ is a phase shift. Equation 1 will be referred to in this paper as the 'constant frequency model.' This expression assumes that the SNR data has a constant frequency ($\frac{4\pi H_0}{\lambda}$). The observations in Figure 2b also show that A is not constant and depends upon elevation angle. However, we use this approximation to minimize the number of parameters required to describe the SNR curve. The simplified, constant frequency and constant amplitude expression does not significantly affect bare ground soil moisture estimations [21]. In this study, we assess how well this simple model applies to vegetation sensing.

It has been shown both in field experiments and a modeling study that A and φ are sensitive to changes in soil moisture content for a bare soil [20][21]. A and φ are found using

least-squares estimation, with H_0 set to the best approximation of the height of the antenna. In practice, the actual antenna height is not known perfectly due to variations in surface elevation surrounding the antenna. For these real data, H_0 is assumed to be the average of bare soil or low vegetation effective reflector height values, calculated using a Lomb-Scargle periodogram, which is described below. For this reason, H_0 is also referred to as the '*a priori* reflector height.'

Other studies have explored how the frequency of the SNR data changes in response to changes in snow depth [24] and water level [26][27]. In these cases, a Lomb-Scargle periodogram (LSP) is used to estimate the dominant frequency of the SNR curve (two examples of LSPs are shown in Fig.2c) [28]. We chose the LSP over a Fourier transform because of its ability to handle unevenly-sampled data. This method of data analysis is not related to the constant frequency model in (1) or estimation of phase or amplitude described above, except in initially establishing the *a priori* reflector height. The peak frequency of the Lomb-Scargle periodogram is converted into an effective reflector height, H_{eff}, using the following equation [29]:

$$H_{eff} = \frac{1}{2} f_m \lambda \qquad (2)$$

Where f_m is the peak frequency of the LSP. Note that H_{eff} is not the same as the *a priori* reflector height, H_0, in Equation 1. However, for soil moisture studies, H_{eff} is very similar to H_0. For sea and snow level studies, H_{eff} varies with reflector distance. This is due to the fact that the permittivity of water (and frequently for snow) is high enough so that the surface of the water or snow acts as a single reflector for the multipath signal, with minimal influence from the underlying medium.

Whether or not a vegetation canopy's permittivity is large enough to act as the dominant reflector is explored in this study. In the case of multiple reflectors, neither the constant frequency model nor the peak frequency of the LSP will adequately characterize the SNR data. Multiple reflectors could result from the soil surface and the top of the vegetation canopy, or from the soil surface and multiple reflections within the canopy. In the case of multiple reflectors, H_{eff} would also not provide complete information about changes in vegetation. This is discussed further in Section 6.

3. Methods

3.1 Vegetation Model

The 1-D, electrodynamic, single-scattering, forward model that we adapted to simulate SNR data in this study was developed in [22] and further explored in [21]. The model was originally developed for bare soil simulations for a flat surface surrounding an antenna. It requires user-defined point soil moisture estimates at specified depths within the soil column. A piecewise, cubic interpolation between depths is used to produce a soil moisture profile that is 20 cm thick, discretized into 1 mm layers, each with its own soil moisture value [21]. In this study, however, we assume a soil column with soil moisture held constant for all depths. This simplification is justified as [21] found that soil moisture variations with depth only minimally impacted SNR metrics.

Soil moisture values are converted into complex permittivity values, using relationships in [6]. [6] describes relationships between volumetric soil moisture and permittivity at L-band frequency for five different soil types using a semi-empirical model. Here, we only report results for a loam soil, as [21] showed that soil type has a negligible impact on SNR metrics.

Our adapted model uses specified vegetation canopy parameters and produces a one dimensional, homogenous permittivity profile of the plant canopy on top of the soil. There is an abrupt contrast between the canopy top and the layer of air above the canopy. [30] found, for a plane-stratified model of vegetation, that such an abrupt transition between the top of the canopy and air could create constructive and destructive interference that is not observed in field data. We tested less-abrupt canopy tops, where we allowed the permittivity of the vegetation canopy to gradually decrease to that of air over different percentages of the canopy height (up to 50% of total canopy height). We conducted this test for canopy heights up to 100 cm and permittivities (real part) up to 1.1. We observed significant differences in SNR metrics only when the transition layer was larger than one wavelength (~24 cm). For these canopies, the largest differences were observed when canopy permittivity was greater than 1.05 (real part), which is higher than for any of our modeled vegetation in this study. Thus, our plane-stratified model would not be suitable for very thick canopies with a large transition layer. Below, we demonstrate that the uniform canopy approximation is suitable for a broad range of vegetation types.

Many studies have used plane-stratified models to simulate emission from vegetation canopies at microwave frequencies (e.g. [31] and [30]). This is in contrast to a geometrical modeling approach, in which each component of the plant canopy, such as stalks and leaves, are modeled by their geometrical shapes (e.g. [32] and [33]). Geometrical modeling is used because, at microwave frequencies, a canopy layer is often considered inhomogeneous and anisotropic [34]. Geometric effects are most important when the components of the canopy, i.e. stalks, leaves, or branches, are the same size or larger than the wavelength of the signal.

Because the wavelength of the GPS L-band signal is approximately 24 cm, which is much longer than X- or C-bands (~3 and 5 cm, respectively), we decided to use a plane-stratified model that does not consider internal canopy geometry. For the range of vegetation types that we tested in this study, geometric components of the canopy were smaller than our wavelength. However, our model might not accurately simulate vegetation types (i.e. corn) that have geometric components of at least 24 cm.

Assuming that structural geometric effects are negligible means that we neglect the coherence loss of the reflected wave due to volume scattering within the plant canopy. However, our model does take into account multiple reflections between one-dimensional layers within the medium if they exist.

At its most basic level, the model uses volumetric soil moisture estimates at specified depths within the soil column and specific vegetation canopy parameters as input to produce theoretical SNR curves. We split our explanation of the model into two general parts: permittivity profile generation and estimation of reflected power received at the antenna.

3.1.1 Permittivity profile generation

For reasons described in the following section, it is necessary for the model to convert the soil moisture depth measurements and vegetation canopy parameters into a 1-D, stratified permittivity profile. Creation of the permittivity layer for the soil is described above.

Vegetation input parameters include vegetation wet weight [kg m^{-2}], dry weight [kg m^{-2}], canopy height [m], vegetation water salinity [‰] and vegetation plant matter density [kg m^{-3}]. The height of the vegetation permittivity layer is thus canopy height.

The permittivity of the vegetation is estimated using a model developed in [35], which requires the frequency (L-band), salinity of vegetation water, and vegetation water content (which we derived from wet and dry weights) to produce a complex permittivity of the vegetation matter. [35] developed the model based on field measurements of corn leaves but found good agreement when the model was extended to different vegetation types. We use their average value of vegetation water salinity for all of our model simulations.

Because the vegetation canopy is actually a mixture of plant matter and air, we use the Complex Refractive Index mixture equation from [36] to get the resulting permittivity of the canopy:

$$\varepsilon_{canopy}^{1/2} = v_{veg}\varepsilon_{veg}^{1/2} + v_{air}\varepsilon_{air}^{1/2} \quad (3)$$

Where: v_{veg} is the volume fraction of vegetation in the canopy, v_{air} is the volume fraction of air in the canopy, ε_{veg} is the permittivity of vegetation, and ε_{air} is the permittivity of air (1.0).

The volume fractions of air and vegetation are estimated by knowing the canopy height and assuming that the density of plant matter is directly proportional to its percent water content.

Table 1 shows the calculated complex permittivities for the prescribed vegetation parameters based on measurements from four field sites, described in detail in Section 3.2. Note that values are very close to that of air, which is expected, given that most plant canopies are comprised mostly of air [37].

3.1.2 Estimation of reflected power received at the antenna

After the combined soil/vegetation permittivity profile is generated, the model estimates both right- and left-handed reflection coefficients that would result from a GPS

multipath signal reflecting out of the soil/vegetation layers at a specified angle of incidence (elevation angle) [38]. The reflection coefficients are combined with the left- and right-handed values of the antenna gain at that elevation angle to get the resulting indirect power. Altering the gain pattern will alter the indirect power. The model uses values of gain for a GPS choke ring antenna typical of our field sites measured in an anechoic chamber.

The procedure described above is repeated for each specified elevation angle in the user specified range. In this paper, we use an elevation angle range of 5-30 degrees, in approximately 0.002 degree increments, which is the range used in previous GPS-IR studies [19] [20]. The interference between the power of the direct and indirect signals makes up the modeled SNR data. A more detailed explanation of model mechanics is described in [22] and will not be included here.

3.2 GPS Data from Field Sites

We use GPS data from four field sites to validate our model. The field sites themselves are described in the next section. All four field sites have a geodetic-quality choke-ring GPS antenna and Trimble NetRS receiver, which collects daily SNR data for each satellite pass. Antennas are identical across sites, though their radiation patterns may vary to some degree, which introduces some small but tolerable uncertainties into our analysis.

On any given day at any site, we used between 8-10 satellite tracks for our analysis of GPS metrics. We used only southern-ascending tracks for our analysis. There were thus between 8-10 satellite tracks with SNR data from which we estimated phase, amplitude, and effective reflector height using procedures described in Section 2. These values were averaged to give one daily phase, amplitude, and reflector height estimate for each site. Standard

deviations of the measurements were also calculated and are shown as error bars in our analyses. Differences in GPS metrics between satellite tracks on one day result from a combination of spatial heterogeneity (satellites rise and set over different areas near the antenna), temporal differences (satellites pass over the antenna at different times of the day), and random noise.

Comparing SNR data across sites necessitated first either normalizing or zeroing each of the three metrics. The magnitude of amplitude is not only affected by soil moisture and vegetation, but also by the satellite transmit power (which is different for each satellite) and the temperature of the receiver. For example, the largest amplitude at the soybean site is different than the largest amplitude at the rangeland site for technical reasons, not because the soil moisture or vegetation conditions differ. To mitigate this issue, we normalized amplitude for each site by dividing each daily-mean amplitude value by the maximum daily-mean amplitude observed at that site. Thus, each site's normalized amplitudes range from 0 to 1, instead of 15-18 volt/volt or 12-16 volt/volt, etc. Because the height of the GPS antenna is different for every site, we only looked at deviations from the *a priori* reflector height. Phase was zeroed at each site. For example, a phase range of 200-300 degrees was reported as 0-100 degrees.

3.3 Vegetation and Soil Moisture Field Data

In order to both validate our model with real data and constrain our model simulations to realistic vegetation conditions, we used field data collected from four sites: an agricultural soybean field in Iowa, an agricultural alfalfa field in Colorado (Fig. 4), a grazed grassland in Oklahoma, and a desert steppe site in Colorado. These sites were selected for this study

because together they represent a wide range of vegetation types, canopy heights, and vegetation water contents. Table 1 contains a summary of the vegetation parameters at the four sites. All four sites are nearly flat – surface elevation varied by less than 0.5 m within the GPS sampling footprint. This allowed us to compare the observed data to model simulations in which the area around the antenna is flat.

In addition to the GPS installation common to all sites (described in the previous section), we installed Campbell Scientific 616 soil moisture probes in the vicinity of each antenna: 5 probes were buried at 2.5 cm depth, 5 at 7.5 cm, and 2 at 20 cm. Probes give estimates of soil moisture every 30 minutes. For model validation, we average the probe estimates at each depth for one day, so that we have daily estimates of soil moisture at the specified depths.

During the growing season, vegetation measurements were taken at each site. At the alfalfa, rangeland, and desert steppe site, measurements were taken approximately every seven days. At the soybean site, measurements were taken every 2-3 weeks throughout the growing season.

Each vegetation measurement included seven samples at random locations within 50 m of the GPS antenna. At each sample location, a 50 x 50 cm grid was thrown on the ground. Canopy height was measured, and all plant material within the grid was cut and weighed. This value was used as vegetation wet weight. The vegetation was subsequently dried in an oven at 50˚C for at least 48 hours and weighed again, yielding vegetation dry weight. Measurements at the soybean field followed a different sampling procedure, but we were able to convert the measurements to our data format. We thus obtained measurements of canopy height, biomass

(dry weight of vegetation), wet weight (total weight of 'wet' vegetation), and gravimetric moisture (weight of water contained in the vegetation divided by the wet weight).

4. Model Validation

For model validation, we used field vegetation and soil moisture data from the four sites as model input. Each vegetation sample for one day was considered to be a separate model input. Thus, each validation point had seven different model simulations, which differed in vegetation parameters. Soil moisture was the daily average value at each depth as described above and was the same for all seven model runs for each day. We averaged phase, amplitude, and reflector height for these simulations and calculated the standard deviation of the metrics. We show the standard deviations as error bars in our validation analysis. These error bars thus represent the variability of model output depending on the spatial variability of real field conditions. Analysis of observed GPS data for model validation is addressed in Section 3.2.

Our results show that the model successfully simulates SNR data for both bare and vegetated conditions. Two examples of observed and modeled SNR data are shown in Fig 5. The observed SNR data are from one satellite track—different satellite tracks would produce slightly different SNR data. The modeled SNR data were produced using soil moisture and vegetation parameters sampled on the same day as the observed data. The model is able to reproduce the amplitude variations with elevation angle that result from the presence of vegetation. The decrease in overall amplitude with the addition of vegetation is also successfully simulated. The simulation of a gradual canopy top (red SNR curve in the figure) introduces only small changes with respect to the homogeneous vegetation layer (blue SNR data). In addition, the SNR data simulated with the gradual canopy top does not match observations.

The modeled and observed periodograms are similar (Figure 5), although the match is not as close as for the SNR data. In particular, the maximum power of the periodogram is less in the observed data than modeled data, for both bare soil and vegetated conditions. This could be a result of colored noise in the observations, due to terrain effects in real environments, or differences in the modeled and observed transmitted power or antenna gain pattern.

Modeled SNR estimations of phase, amplitude, and effective reflector height show good agreement with those observed in the field (Fig.6). For all three relationships, the simulated-observed pairs fall close to the 1:1 line. Figure 6 shows how amplitude changes as vegetation grows, similar to what is shown in the time series in Figure 2. Highest values of normalized amplitude correspond to either (1) the sites with the least vegetation (steppe/rangeland); or (2) the agricultural sites at times in the year when there was little vegetation present. Both simulated and observed amplitude values are less than 0.4 during peak growth at the soybean and alfalfa site. In Figure 6, low values of phase correspond to maximum vegetation. Phase variations for rangeland and steppe sites are limited to 50 degrees on all dates. The greatest range of phase shift is simulated and observed at the alfalfa site (200 degrees). Figure 6 also shows that effective reflector height, for the most part, does not change significantly throughout the growing season. Only large changes are seen at the alfalfa site, and the model simulates this as well.

Error bars for some validation points are quite large. Large vertical error bars represent the standard deviation of retrievals for all satellite tracks on one particular day. Because satellites rise and set at different times during the day and over different areas near the GPS antenna, each satellite retrieval will be inherently different due to spatial and temporal

variability. Large horizontal error bars represent the standard deviation of model output for a given day. Because vegetation at some sites varies spatially, the field data yields very different inputs to the model, so it is expected that the model outputs should vary considerably, especially for the rangeland and steppe sites.

Calculated SNR metrics from modeled data with a gradual canopy top did not differ significantly from the homogeneous canopy, thus we do not show these results.

5. How GPS metrics respond to change in vegetation

We now analyze how GPS metrics should respond to changes in vegetation extent. We no longer used each field sample as model input, as was used for validation of the model in the previous section. Instead, we used field data to derive relationships between vegetation wet weight and height and vegetation wet weight and dry weight for each of the four sites. This was done using a linear regression of field data. Thus, although we report our results in terms of wet weight, relationships would be the same for canopy height and dry weight as well, since heights were assumed to be linearly proportional to wet weights. In general, the regressions showed good relationships between wet weight, dry weight, and height. The only exception was the rangeland site, which had an r^2 value between height and wet weight of only 0.15, which we attribute to the sparse and inhomogeneous vegetation at the site. Otherwise, r^2 values for wet weight and height or wet weight and biomass were greater than 0.5, with the agricultural sites having the highest r^2 values. We also used the average vegetation percent water content for each site for each simulation, even though Table 1 shows significant variations. Sensitivity of SNR metrics to percent water content is investigated below. We also assumed that the density of plant matter was directly proportional to its percent water content. Thus, if the sample was

75% water on a wet weight basis, this translated to a density of 750 kg m^{-3}. Obviously, these relationships are generalized and not descriptive of every plant canopy. However, by including multiple sites with different canopy water contents and relationships between field parameters, we consider our analysis to encompass the majority of non-forested vegetation canopies.

For each site, we increased the modeled vegetation wet weight from 0 kg m^{-2} to 4 kg m^{-2}, even though the rangeland and desert steppe site would never realistically have this much vegetation. For these two sites, we extrapolate values out to 4 kg m^{-2} using the same linear regressions from field data as described above. For relative scale, a field of corn could contain in excess of ~6 kg m^{-2} of vegetation material [4] whereas a typical grassland would average around 0.4 kg m^{-2} [39]. For each modeled canopy, we varied soil moisture between 0.05 and 0.40 cm^3 cm^{-3} to quantify how soil moisture could influence the ability of an SNR metric to sense changes in a vegetation canopy. We then estimated phase, amplitude, and effective reflector height for each model simulation. For our model simulations, we kept the height of the antenna at 2.4 m for all four sites.

The relationship between SNR metrics and vegetation wet weight for the four sites, given a dry underlying soil (SMC = 0.05), is shown in Fig 7. For these sites, the realistic vegetation wet weights are shown by the solid line, and extrapolated relationships are shown by the dashed line.

As Figure 7 illustrates, both phase and amplitude decrease in a mostly linear fashion as vegetation wet weight increases, until about 1 kg m^{-2}. Once the wet weight of vegetation has exceeded this value, there is no clear relationship between these two metrics and wet weight.

Furthermore, the complex relationship past 1 kg m^{-2} also becomes site dependent. The simulated differences between sites are due to the site-specific relationships between height, vegetation water content, and density. Effective reflector height oscillates with increasing wet weight and is also site dependent. From this analysis alone, it appears that either phase or amplitude could be used to predict changes in vegetation wet weight up to 1 kg m^{-2}. Past this value, the relationship between wet weight and these two metrics has less predictive value.

The effects of both soil moisture and vegetation wet weight on GPS metrics for the four sites are shown in Fig. 8. In this figure, we did not extend our analysis out to 4 kg m^{-2} for the rangeland and the steppe sites. We did this to clarify the role that soil moisture plays in estimating vegetation wet weight. In this figure, the solid line indicates the response of metrics to vegetation with a saturated underlying soil (SMC = 0.40). The dotted line indicates the response of metrics to vegetation with a dry underlying soil (SMC = 0.05), equivalent to what is shown in Fig. 7. The shaded region thus indicates the effect of soil moisture on metrics for a given vegetation canopy.

This analysis shows that once soil moisture is allowed to vary, phase is no longer a robust indicator of vegetation change for low vegetation extents (wet weight < 1 kg m^{-2}). At low vegetation extents, phase is nearly as sensitive to changes in soil moisture as it is to changes in vegetation. The potential error in estimating vegetation from phase alone is thus large (on the order of 0.5 kg m^{-2}) if soil moisture is unknown. Similarly, estimating soil moisture when vegetation wet weight is unknown would introduce significant error. This error has two components: (1) vegetation affects phase; and (2) the sensitivity of phase to soil moisture depends on the overlying vegetation canopy. The arrows in Figure 8 show that this relationship

is complex, in particular the sensitivity of phase to soil moisture does not simply decrease with increasing vegetation. Although the sensitivity changes, the relationship between phase and soil moisture at a specific vegetation wet weight is nearly linear. Thus, the most accurate soil moisture estimations would require first estimating vegetation amount, and then applying the relationship between phase and soil moisture for the estimated vegetation state.

Amplitude, however, is not as sensitive to soil moisture changes. This was also shown in [21] for a modeled bare soil. Thus, for low vegetation extents (wet weight < 1 kg m^{-2}), it is possible to use amplitude as a proxy for vegetation change. There is still uncertainty associated with this metric due to soil moisture, on the order of 0.1 – 0.2 kg m^{-2}. For low vegetation wet weights, such as at the steppe site, this uncertainty could translate to an over- or under-estimation of vegetation of up to 20%.

Figure 8 shows, as in the previous figure, that effective reflector height is not a good indicator of vegetation change. This is despite the fact that soil moisture has a negligible impact on reflector height as compared to the effect from vegetation. The oscillatory effects seen in reflector height for some vegetation canopies are not due to errors in the Lomb-Scargle periodogram. Rather, once vegetation extent is high, the dominant peak in the periodogram is hardly distinguishable from other, smaller peaks. Thus the peak power will sometimes be contained in a peak at one frequency and at other times in a peak at a different frequency. This causes the apparent jumps in effective reflector height. This should be interpreted as the SNR data no longer having one distinguishable frequency. We explain and quantify this effect further in Section 6.

Previous GPS-IR studies used 5-30 degrees in the estimation of phase and amplitude. However, because reflection coefficients are dependent upon elevation angle and should be highest at grazing (low) angles, it is reasonable to assume that certain elevation angles are more sensitive to changes in vegetation than others. We used the model and field data to see whether restricting amplitude analysis to 5-15 degrees would improve its relationship with vegetation wet weight. For this analysis, we chose to do a linear interpolation between the vegetation field samples for the soybean site since there were only five original sample points. This interpolation was justified due to the monotonically increasing relationship over time seen in field data (see Fig. 2a for this relationship).

In general, the model indicated that using 5-15 degrees would actually be worse in vegetation estimation than using 5-30 degrees (Fig. 9a). This is because, even though the magnitude of amplitude change throughout the growing season was greater using 5-15 degrees, the relationship with wet weight was even more non-linear. This effect is seen both in field and modeled data (Fig. 9). For comparison, the analogous model and field results using 5-30 degrees are shown in Fig. 9c-d. These data indicate that using 5-15 degrees for amplitude estimation does not increase the potential of this metric to successfully model changes in vegetation past 1 kg m^{-2} of wet weight. There are significant differences in the relationship between wet weight and modeled results. For example, the first notable dip in amplitude occurs at 1 kg m^{-2} in the model but at 0.7 kg m^{-2} in real data. These differences arise from the simplifications made in the model as well as errors in field sampling, which are explained in the beginning of this section. We tried other elevation angle ranges, and all yield similar results to

those shown. We conclude that there are no distinct advantages to using a more restricted elevation angle range than 5-30 degrees.

6. Quantifying when the constant frequency model is appropriate

Phase and amplitude estimates using the constant frequency model of (1) are only valid if the frequency of the SNR curve is approximately equal to the height of the antenna, or the '*a priori* reflector height.' Figure 10 (b,d) shows that this is not the case for highly-vegetated environments, nor is the effective reflector height always close to the height of the vegetation. As vegetation grows, the following may happen:

1. The dominant frequency shifts away from the *a priori* reflector height (shifting).
2. The dominant frequency becomes less powerful in relation to other frequencies (spreading and dampening). Conversely, other frequencies become more powerful in relation to the bare soil frequency.

Together, these two effects lead to errors in estimation of phase and amplitude and ultimately a mischaracterization of the SNR curve. Figure 10 (a,c) shows modeled SNR curves overlain by the curve generated using the constant frequency model of (1) and the least-squares estimates of phase and amplitude. We refer to this data as the reconstructed data. It is apparent that least-squares estimation fails when the SNR data is not adequately described by (1).

We describe how the constant frequency model begins to mischaracterize the SNR curve as vegetation extent increases using two general methods. First, we look at two different metrics that characterize how the Lomb-Scargle peak frequency (effective reflector height) and its power change as vegetation extent increases. These metrics include the fraction of power in

the periodogram that remains near the antenna height/bare soil frequency as well as the fraction of power in the dominant periodogram peak.

The shifting and spreading of the frequency of the SNR data as vegetation water content increases are shown in Figure 11a and b. Figure 11a shows how much power of the Lomb-Scargle periodogram is still at or near the effective reflector height for a bare soil, as a function of vegetation wet weight. This shows the effect of the dominant frequency(cies) shifting. Figure 11b shows how much power is contained within the dominant frequency peak within the periodogram, as a function of vegetation wet weight. This shows the spreading and dampening effect that vegetation has on the frequency of the SNR curve.

Second, we calculate the r^2 value between the actual SNR data and the reconstructed data as a measure of misfit between the two. We report results using both modeled SNR data as well as ones from field data.

The mean r^2 value for the relationship between the actual and reconstructed SNR data is shown in Fig. 12. It is apparent that once vegetation wet weight increases beyond 1 kg m^{-2}, the misfit between the actual and 'reconstructed' data increases dramatically, shown by a much lower r^2 value. This may help explain why neither phase nor amplitude show a clear relationship between increases in vegetation wet weight beyond this value. Thus, phase and amplitude estimates for vegetation exceeding 1 kg m^{-2} should not be expected to be representative of their corresponding SNR curves.

7. Conclusions:

An electrodynamic forward model developed and validated in this study reproduces basic changes in GPS SNR data associated with vegetation canopies. This includes changes in

SNR amplitude at different elevation angles, changes in the pattern of the Lomb-Scargle Periodogram, and changes in SNR metrics. These changes were well simulated across a range of vegetation wet weights at four field sites.

The vegetation model shows that, once vegetation canopy wet weight exceeds 1 kg m^{-2}, SNR phase and amplitude (estimated using 5-30 degrees) alone cannot be used to reliably retrieve vegetation parameters. Effective reflector height is never a consistent or reliable indicator of vegetation change. Using data from lower elevation angles, such as 5-15 degrees, does not improve the capability of amplitude to sense vegetation change when vegetation extent is high.

When vegetation wet weight is below 1 kg m^{-2}, it could be possible to estimate wet weight using phase or amplitude, if surface soil moisture is known. When it is not known, amplitude is the only reliable metric to use to estimate vegetation wet weight. Still, the error introduced from unknown soil moisture could be on the order of 0.1-0.2 kg m^{-2}. For vegetation canopies that are less than 1 kg m^{-2}, this translates to an error of 10-20%. However, if the goal is to compare vegetation across sites, this error is small.

A vegetation canopy can decrease the presence of one dominant frequency in the SNR curve, and so the constant frequency model that is used to estimate phase and amplitude fails to adequately characterize the SNR curve when there is significant vegetation cover. There is a sharp decrease in the constant frequency model's ability to characterize the SNR curve once vegetation wet weight exceeds 1 kg m^{-2}. Thus, a method that could quantify or include variation of frequency with elevation angle and the growth of vegetation would likely be more successful at describing changes in the vegetation canopy. The development of such a method or the use

of an inverse procedure should be the subject of future efforts if we wish to successfully quantify high vegetation extent using SNR data.

Acknowledgements

The authors would like to thank Brian Hornbuckle of Iowa State University, Tyson Ochsner of Oklahoma State University, UNAVCO, and the helpful comments from the reviewers. This work was funded in part from AGS-0935725.

References

[37] Attema, E. P. W., & Ulaby, F. T. (1978). Vegetation modeled as a water cloud. *Radio Sci*, *13*(2), 357–364. doi:10.1029/RS013i002p00357

[29] Axelrad, P., Larson, K. M., & Jones, B. (2005). Use of the correct satellite repeat period to characterize and reduce site-specific multipath errors. *ION GNSS 18th International Technical Meeting of the Satellite Division*, (September), 2638–2648.

[2] Brown, M. E., De Beurs, K. M., & Marshall, M. (2012). Global phenological response to climate change in crop areas using satellite remote sensing of vegetation, humidity and temperature over 26 years. *Remote Sens Environ*, *126*, 174–183. doi:10.1016/j.rse.2012.08.009

[11] Cardellach, E., Ruffini, G., Pino, D., Rius, A., Komjathy, A., & Garrison, J. L. (2003). Mediterranean Balloon Experiment: ocean wind speed sensing from the stratosphere, using GPS reflections. *Remote Sens Environ*, *88*(3), 351–362. doi:10.1016/S0034-4257(03)00176-7

[13] Cardellach, E., Fabra, F., Rius, A., Pettinato, S., D'Addio, S. (2012). Characterization of dry-snow sub-structure using GNSS reflected signals. *Remote Sens Environ*, *124*, 122-134.

[21] Chew, C., Small, E., Larson, K., Zavorotny, V. (in press). Effects of Near-Surface Soil Moisture on GPS SNR Data: Development of a Retrieval Algorithm for Soil Moisture. *IEEE T Geosci Remote*. doi: 10.1109/TGRS.2013.2242332

[39] Dasgupta, S., & Qu, J. J. (2009). Soil adjusted vegetation water content retrievals in grasslands. *Int J Remote Sens*, *30*(4), 1019–1043. doi:10.1080/01431160802438548

[23] Egido, A., Caparrini, M., Ruffini, G., Paloscia, S., Santi, E., Guerriero, L., … Floury, N. (2012). Global Navigation Satellite Systems Reflectometry as a Remote Sensing Tool for Agriculture. *Remote Sens*, *4*(12), 2356–2372. doi:10.3390/rs4082356

[8] Ferrazzoli, P., Guerriero, L., & Solimini, D. (2000). Simulating Bistatic Scatter From Surfaces Covered With Vegetation. *J Electromagnet Wave*, *14*, 233–248.

[38] Fuks, I. M., & Voronovich, A. G. (2000). Wave diffraction by rough interfaces in an arbitrary plane-layered medium. *Wave Random Media*, *10*, 37–41.

[12] Gleason, S., Hodgart, S., Gommenginger, C., Mackin, S., Adjrad, M., & Unwin, M. (2005). Detection and Processing of bistatically reflected GPS signals from low Earth orbit for the purpose of ocean remote sensing. *IEEE T Geosci Remote*, *43*(6), 1229–1241. doi:10.1109/TGRS.2005.845643

[9] Gleason, S., Lowe, S., & Zavorotny, V. (2009). Remote Sensing Using Bistatic GNSS Reflections. In *GNSS Applications and Methods*. Norwood: Artech House.

[6] Hallikainen, M. T., Ulaby, F. T., Dobson, M. C., El-Rayes, M. a, & Wu, L.-K. W. L.-K. (1985). Microwave Dielectric Behavior of Wet Soil-Part 1: Empirical Models and Experimental Observations. *IEEE T Geosci Remote*, *GE-23*(1), 25–34.

[4] Jackson, T. (2004). Vegetation water content mapping using Landsat data derived normalized difference water index for corn and soybeans. *Remote Sens Environ*, *92*(4), 475–482. doi:10.1016/j.rse.2003.10.021

[40] Jacobson, M. (2008). Dielectric-covered ground reflectors in GPS multipath reception—Theory and measurement. *IEEE Geosci Remote Sens*, *5*(3), 396-399.

[32] Karam, M. A., Fung, A. K., Lang, R. H., & Chauhan, N. S. (1992). Model for Layered Vegetation. *IEEE T Geosci Remote Sens*, *30*(4), 767–784.

[10] Komjathy, A., Zavorotny, V. U., Axelrad, P., Born, G. H., & Garrison, J. L. (2000). GPS Signal Scattering from Sea Surface : Wind Speed Retrieval Using Experimental Data and Theoretical Model. *Remote Sens Environ*, *73*, 162–174.

[20] Larson, K. M., Braun, J. J., Small, E. E., Zavorotny, V. U., Gutmann, E. D., & Bilich, A. L. (2010). GPS Multipath and Its Relation to Near-Surface Soil Moisture Content. *IEEE J Sel Top Appl*, *3*(1), 91–99.

[26] Larson, K. M., Löfgren, J. S., & Haas, R. (2013). Coastal sea level measurements using a single geodetic GPS receiver. *Adv Space Res*, *51*(8), 1301–1310. doi:10.1016/j.asr.2012.04.017

[24] Larson, K. M., & Nievinski, F. G. (2012). GPS snow sensing: results from the EarthScope Plate Boundary Observatory. *GPS Solut*, *17*(1), 41–52. doi:10.1007/s10291-012-0259-7

[27] Larson, K. M., Ray, R. D., Nievinski, F. G., & Freymueller, J. T. (2013). The Accidental Tide Gauge: A GPS Reflection Case Study From Kachemak Bay, Alaska. *IEEE Geosci Remote S, 10*(5), 1200–1204. doi:10.1109/LGRS.2012.2236075

[19] Larson, K. M., Small, E. E., Gutmann, E., Bilich, A., Axelrad, P., & Braun, J. (2008). Using GPS multipath to measure soil moisture fluctuations: initial results. *GPS Solut, 12*(3), 173–177. doi:10.1007/s10291-007-0076-6

[25] Larson, K. M., Small, E. E., Gutmann, E. D., Bilich, A. L., Braun, J. J., & Zavorotny, V. U. (2008). Use of GPS receivers as a soil moisture network for water cycle studies. *Geophys Res Lett*, *35*(24), 1–5. doi:10.1029/2008GL036013

[30] Lee, K., Chawn Harlow, R., Burke, E. J., & Shuttleworth, W. J. (2002). Application of a plane-stratified emission model to predict the effects of vegetation in passive microwave radiometry. *Hydrol Earth Syst Sci*, *6*(2), 139–152. doi:10.5194/hess-6-139-2002

[31] Mo, T., Choudhury, B. J., Schmugge, T. J., Wang, J. R., & Jackson, T. J. (1982). A Model for Microwave Emission from Vegetation-Covered Fields. *J Geophys Res*, *87*(1), 11229–11237.

[3] Moran, M. S., Inoue, Y., & Barnes, E. M. (1997). Opportunities and limitations for image-based remote sensing in precision crop management. *Remote Sens Environ*, *61*(3), 319–346.

[36] Nelson, S. O. (1991). Dielectric properties of agricultural products-measurements and applications. *IEEE T Instrum Meas*, *41*(1), 385–387.

[18] Nievinski, F., Larson, K. (2013). Forward modeling of GPS multipath for near-surface reflectometry and positioning applications. *GPS Solut,* (in press).

[5] Pan, M., Sahoo, a. K., Wood, E. F., Al Bitar, A., Leroux, D., & Kerr, Y. H. (2012). An Initial Assessment of SMOS Derived Soil Moisture over the Continental United States. *IEEE J Sel Top Appl*, *5*(5), 1448–1457. doi:10.1109/JSTARS.2012.2194477

[14] Rodriguez-Alvarez, N., Aguasca, A., Valencia, E., Bosch-Lluis, X., Ramos-Perez, I., Park, H., Camps, A., Vall-Ilossera, M. (2011). Snow monitoring using GNSS-R techniques. *Geoscience and Remote Sensing Symposium,* 4375-4378.

[16] Rodriguez-Alvarez, N., Bosch-Lluis, X., Camps, a., Aguasca, a., Vall-llossera, M., Valencia, E., … Park, H. (2011). Review of crop growth and soil moisture monitoring from a ground-based instrument implementing the Interference Pattern GNSS-R Technique. *Radio Sci*, *46*(6), n/a–n/a. doi:10.1029/2011RS004680

[15] Rodriguez-alvarez, N., Bosch-lluis, X., Park, H., & Vall-llossera, M. (2012). Vegetation Water Content Estimation Using GNSS Measurements. *IEEE Geosci Remote Sens*, *9*(2), 282–286.

[33] Schwank, M., Mätzler, C., Guglielmetti, M., & Flühler, H. (2005). L-Band Radiometer Measurements of Soil Water Under Growing Clover Grass. *IEEE T Geosci Remote*, *43*(10), 2225–2237.

[17] Small, E., Larson, K., Braun, J. (2010). Sensing vegetation growth using reflected GPS signals. *Geophys Res Lett, 37*(L12401).

[35] Ulaby, F. T., & El-Rayes, M. a. (1987). Microwave Dielectric Spectrum of Vegetation - Part II: Dual-Dispersion Model. *IEEE T Geosci Remote*, *GE-25*(5), 550–557.

[34] Ulaby, Fawwaz T, & Wilson, E. A. (1985). Microwave Attenuation Properties of Vegetation Canopies. *IEEE T Geosci Remote*, *GE-23*(5), 746–753.

[7] Wang, J. R., Engman, E. T., Shiue, J. C., & Rusek, M. (1986). Observations of Microwave Dependence on Soil Moisture , Surface Roughness , and Vegetation Covers. *IEEE T Geosci Remote*, *GE-24*(4), 510–516.

[28] W.H. Press, S.A. Teukolsky, W.T. Vetterling, B.P. Flannery (1992). *Numerical Recipes in Fortran 77* (Vol.1 2nd ed.) New York, NY: Cambridge University Press. pp. 569-573.

[22] Zavorotny, V. U., Larson, K. M., Braun, J. J., Small, E. E., Gutmann, E. D., & Bilich, A. L. (2010). A Physical Model for GPS Multipath Caused by Land Reflections : Toward Bare Soil Moisture Retrievals. *IEEE J Sel Top Appl*, *3*(1), 1–11.

[1] Zhang, X., Friedl, M. a, Schaaf, C. B., Strahler, A. H., Hodges, J. C. F., Gao, F., … Huete, A. (2003). Monitoring vegetation phenology using MODIS. *Remote Sens Environ*, *84*(3), 471–475.

Figures

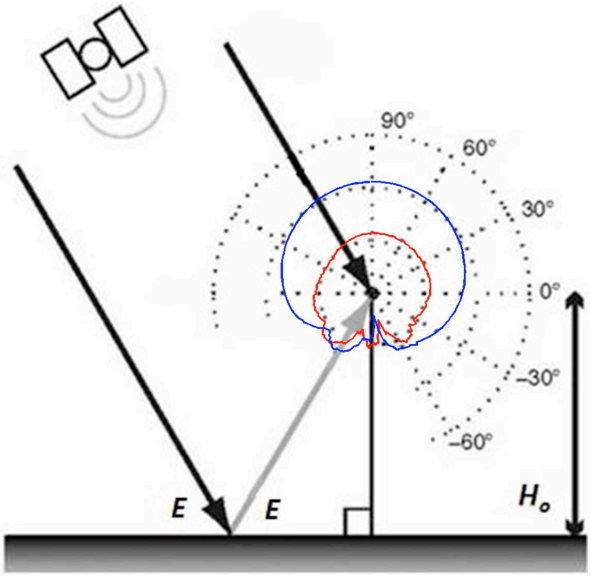

Figure 1: Geometry of a multipath signal, for antenna height (H_o) and satellite elevation angle (E). Bold black lines represent the direct signal transmitted from the satellite. The gray line is the reflected signal from the ground. The antenna's phase center is shown as the small dot. The blue line (higher gain) represents the RHCP gain of the antenna. The red line (lower gain) represents the LHCP gain of the antenna. The radial distance between the antenna phase center and the solid line represents the strength of the antenna gain, in dB.

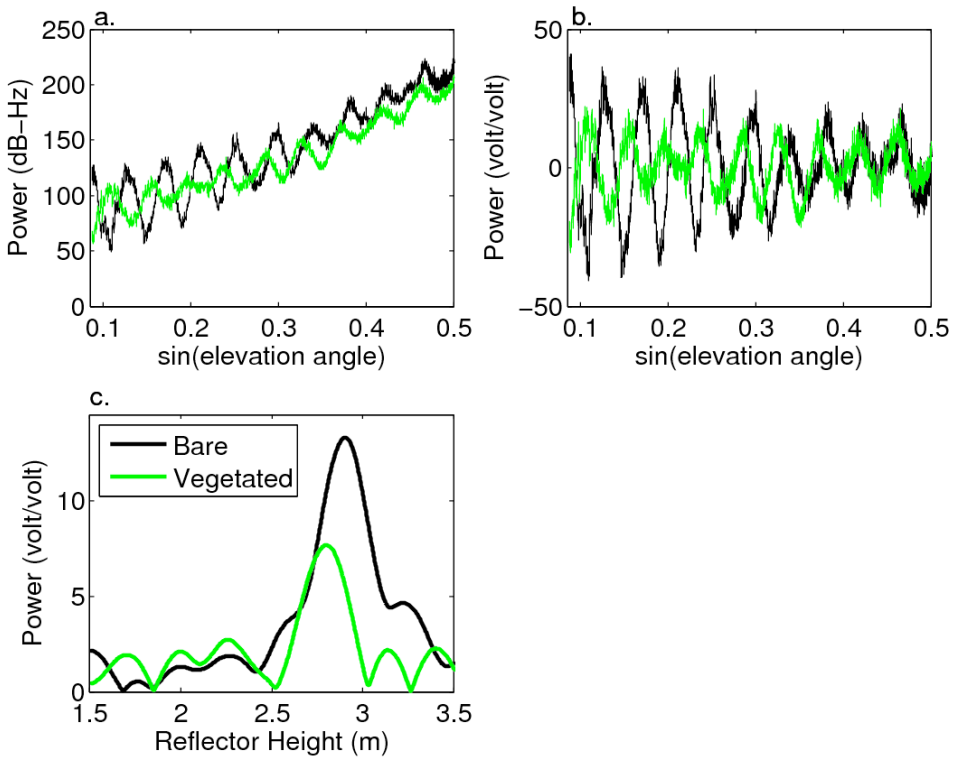

Figure 2: Black lines indicate data retrieved when ground was bare. Green lines indicate data retrieved when ground had 2.5 kg m-2 of vegetation present. Data is from the soybean site. (a) SNR data from one satellite on two separate days. Data still has the direct component. (b) Same SNR data as from panel a., but with the direct component removed and transformed to a linear scale. (c) Lomb-Scargle periodograms indicating the frequency content of SNR curves in panel b.

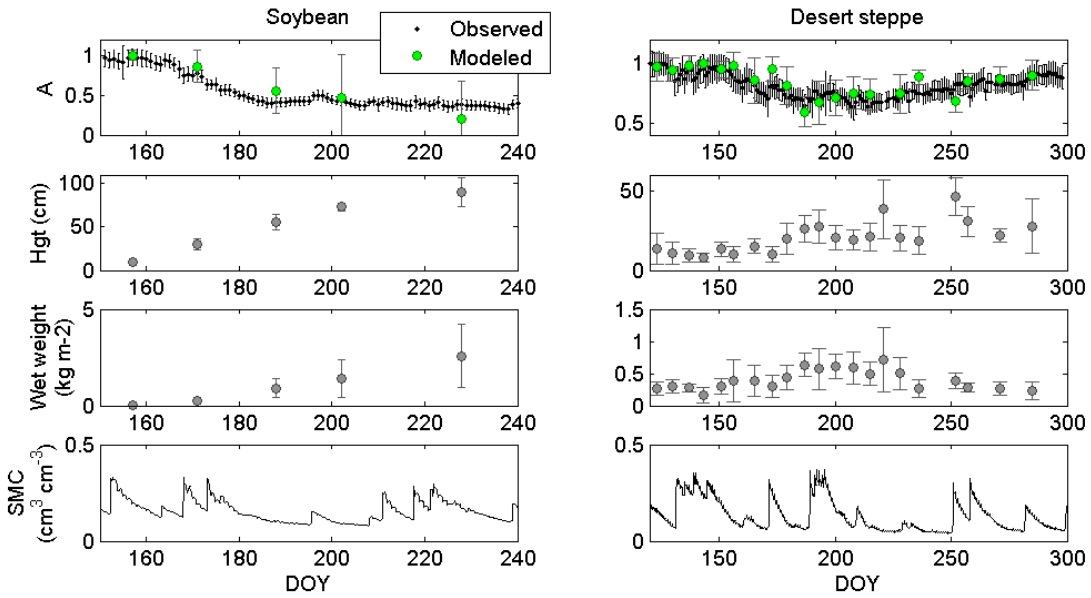

Figure 3: (a) Time series of data for the soybean field in 2012. Top panel is the average and standard deviation of SNR amplitude for all satellites on a given day (black dots) with the model simulations using field data as input (green dots). Below are measurements of canopy height, vegetation wet weight, and 0-5 cm average soil moisture, respectively. (b) Same as panel a., except for the desert steppe site in 2011. Note the scales of the y-axes for field data between the panels are not the same.

Figure 4: Photo from the alfalfa field in Colorado, showing the GPS antenna, receiver box, and solar panel typical of all field sites in this study.

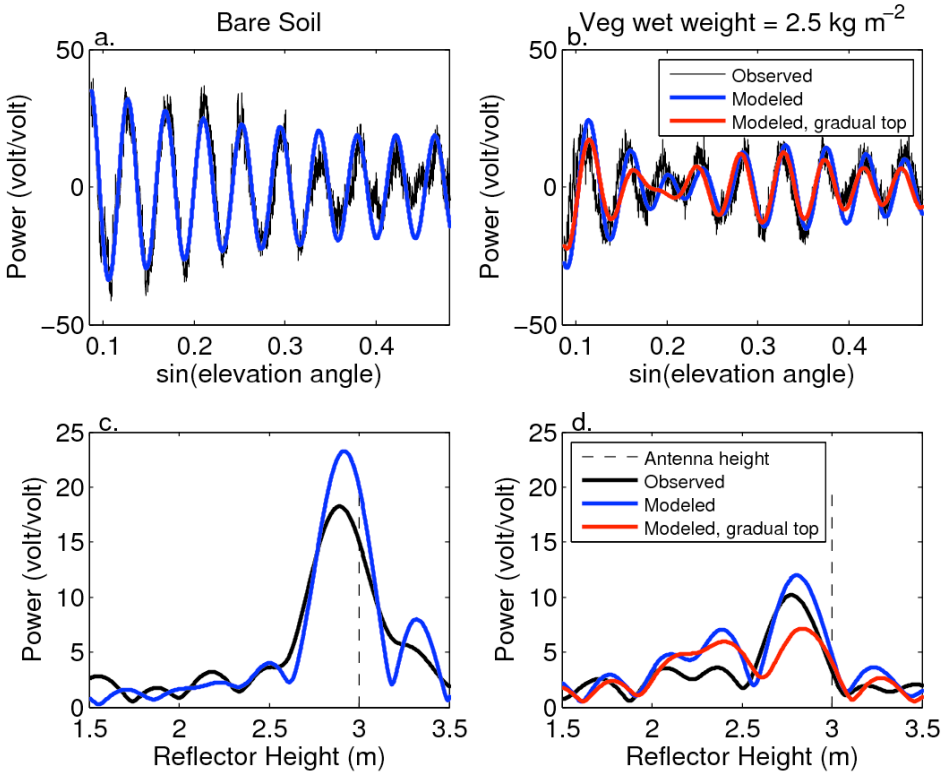

Figure 5: (a) Black line is SNR data from one satellite passing over the soybean site when ground was bare. Blue line is one modeled representation with a soil moisture of 0.15, using field inputs from the same day as the observed data. (b) Same as in a., except for when the

vegetation was at its maximum extent (vegetation wet weight 2.5 kg m-2). The red line uses the same field inputs as the blue line, except also with a gradual canopy top that begins to thin out at 90% height. (c) Corresponding Lomb-Scargle periodograms for the curves in a. (d) Corresponding Lomb-Scargle periodograms for the curves in b.

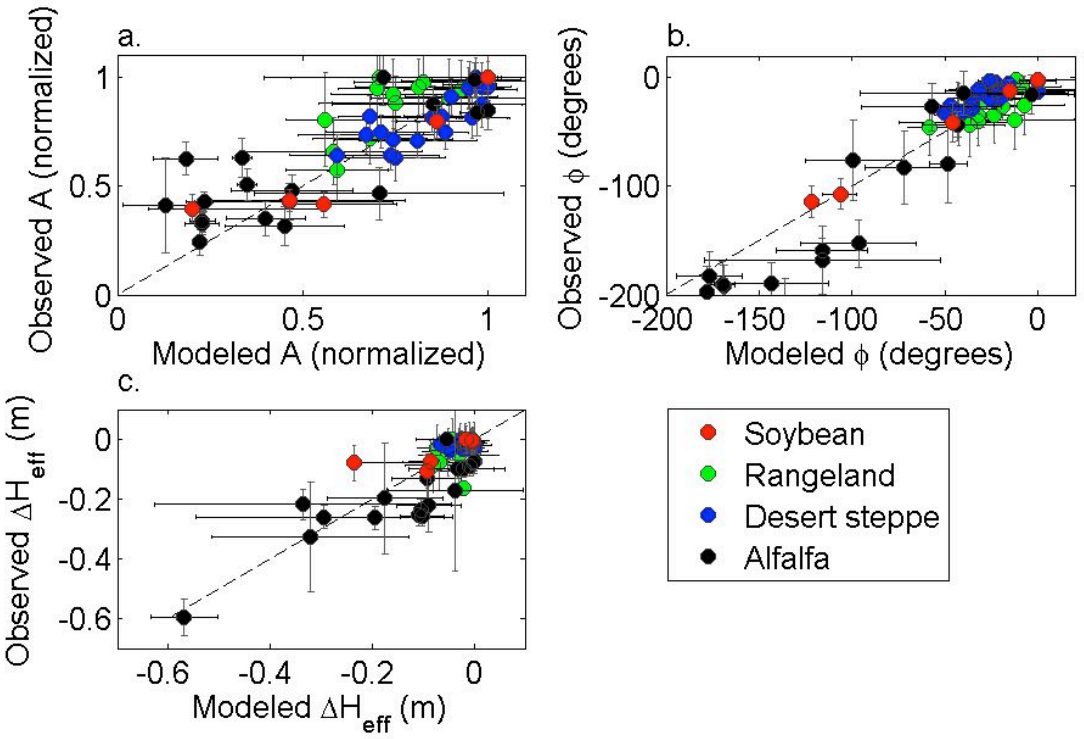

Figure 6: Modeled versus observed estimations of (normalized) amplitude, phase, and effective reflector height for the four sites. Dashed lines are 1:1 relationships.

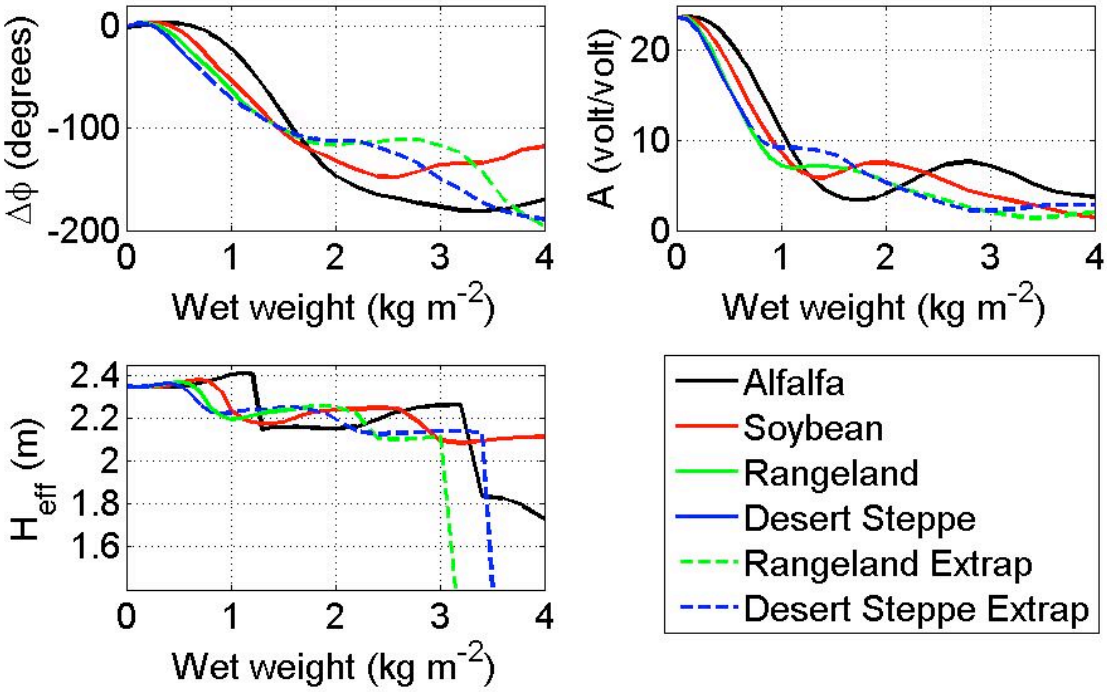

Figure 7: Relationship between modeled SNR metrics and vegetation wet weight for the four sites. The solid lines indicate realistic vegetation conditions for the site. Dashed lines are extrapolated values.

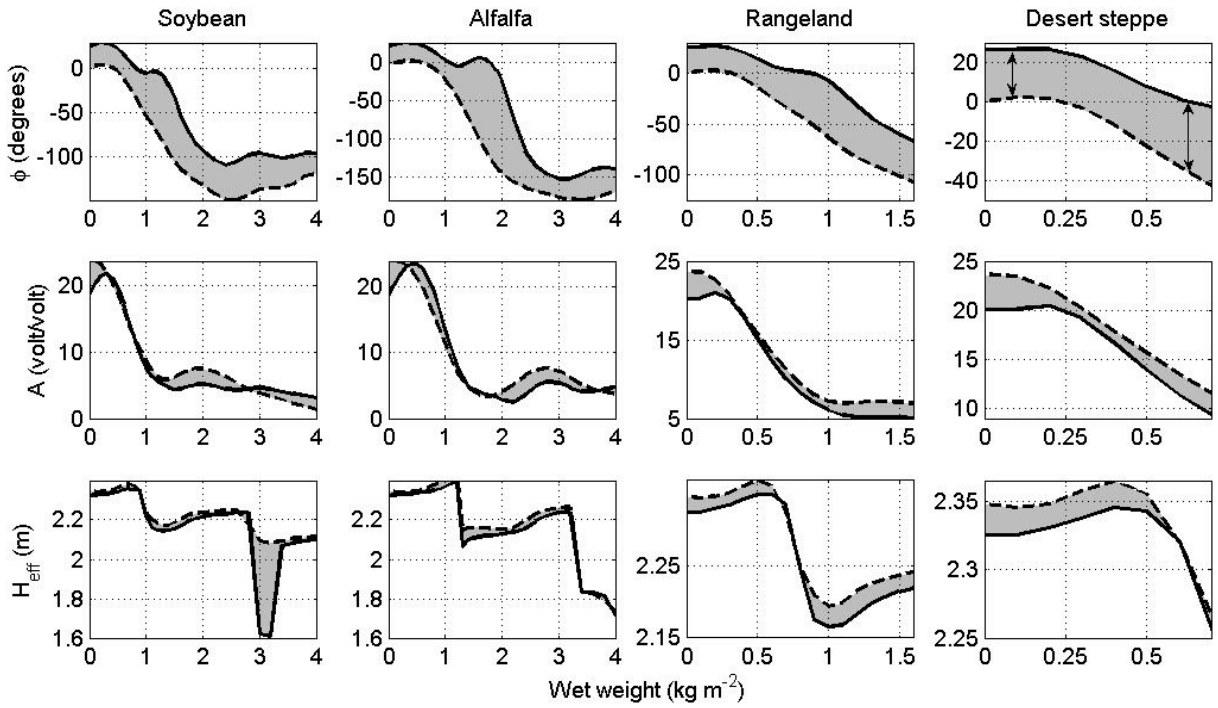

Figure 8: Relationship between vegetation wet weight and SNR metrics for the four sites, with varying underlying soil moisture. The dashed line represents a soil moisture value of 0.05. The solid line represents a soil moisture value of 0.40. The grey area is thus the variation of metrics possible due to soil moisture, for a given vegetation canopy. As the arrows in the top right plot indicate, the sensitivity of phase to soil moisture depends on the amount of overlying vegetation. Corresponding arrows are not included in the other plots in the top row for clarity.

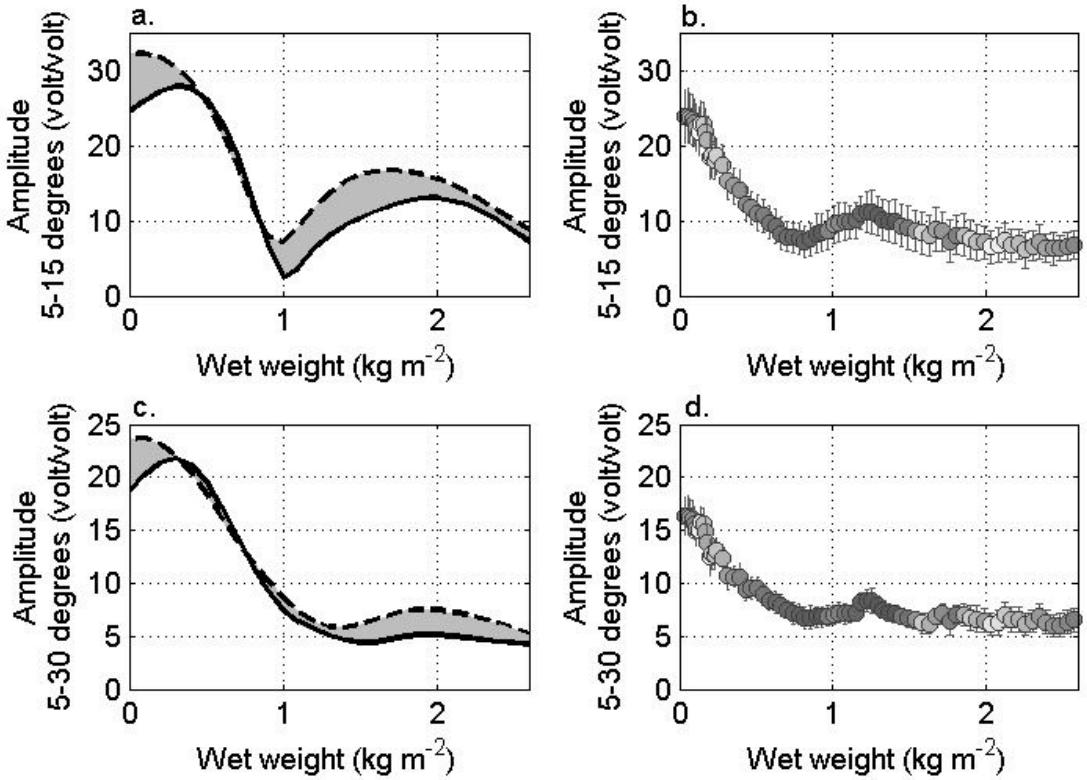

Figure 9: The relationship between vegetation wet weight and amplitude, calculated using an elevation angle range of either 5-15 degrees (top row), or 5-30 degrees (bottom row). Panels (a) and (c) are modeled using relationships from the soybean site. These panels also show the range of responses of amplitude due to different underlying soil moisture, in accordance with Figure 8. Panels (b) and (d) are real, interpolated vegetation data from the soybean site. Dots for the observed data are color coded by relative soil moisture, with lighter values indicating dryer values.

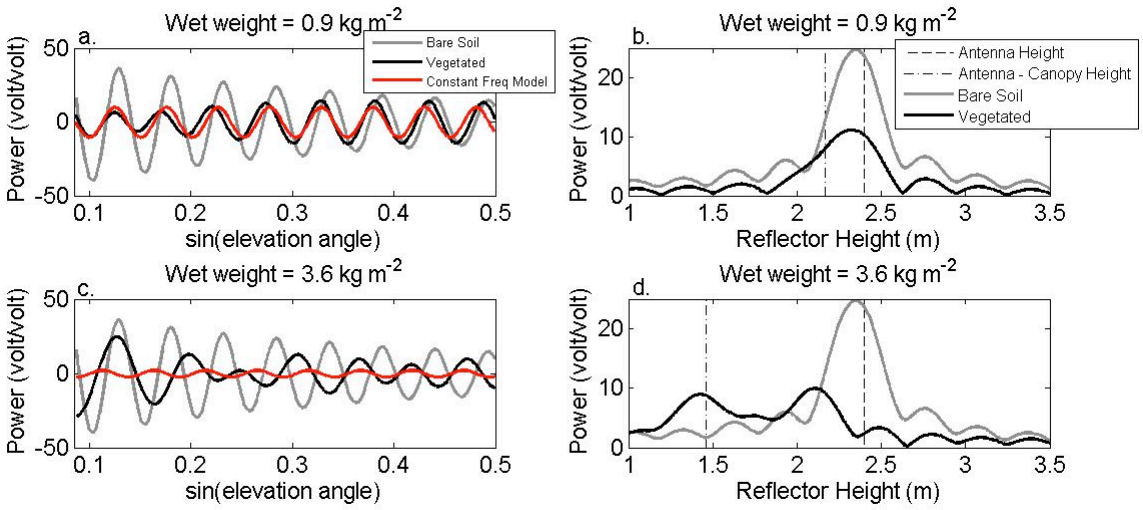

Figure 10: (a) A modeled curve with vegetation wet weight = 0.9 kg m^{-2} (black) and the 'reconstructed' curve (red) generated using the constant frequency model and SNR metrics estimated from the black curve. A modeled curve for bare soil is in grey for reference. (b) Lomb-Scargle periodogram (black) for the simulated curve in panel a. The antenna height is the dashed line, and the distance between the antenna and the canopy top is the dash-dotted line. The grey periodogram is for the bare soil curve in panel a. (c and d) Same as in panels a. and b., except for vegetation wet weight = 3.6 kg m^{-2}.

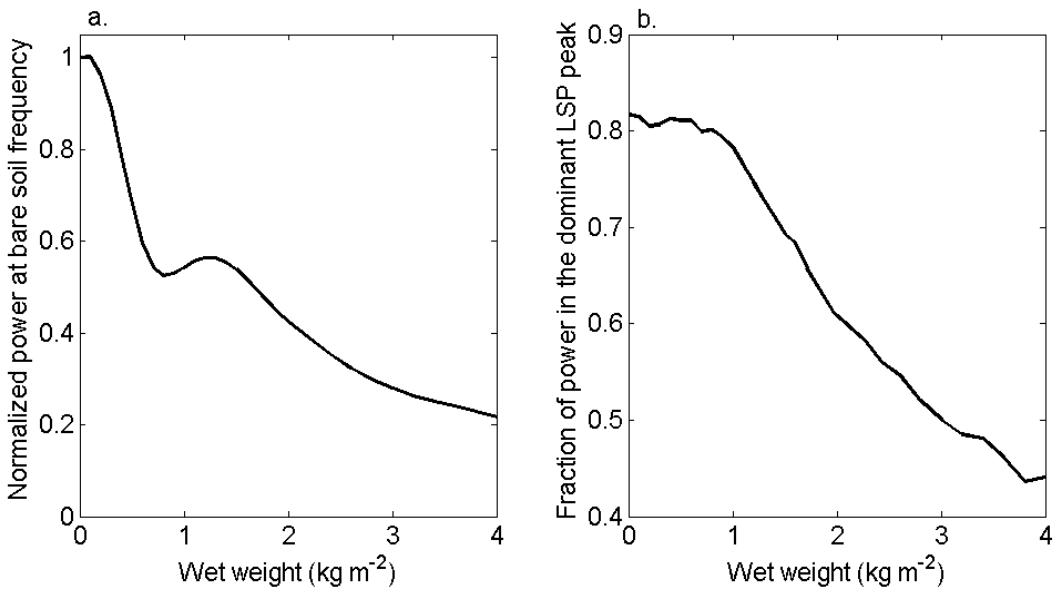

Figure 11: (a) As vegetation wet weight increases, the amount of power in the Lomb-Scargle periodogram at the bare soil frequency decreases. Black line is the average relationship for all sites (normalized with respect to the maximum value). (b) As vegetation wet weight increases, the power contained in the dominant peak of the Lomb-Scargle periodogram decreases.

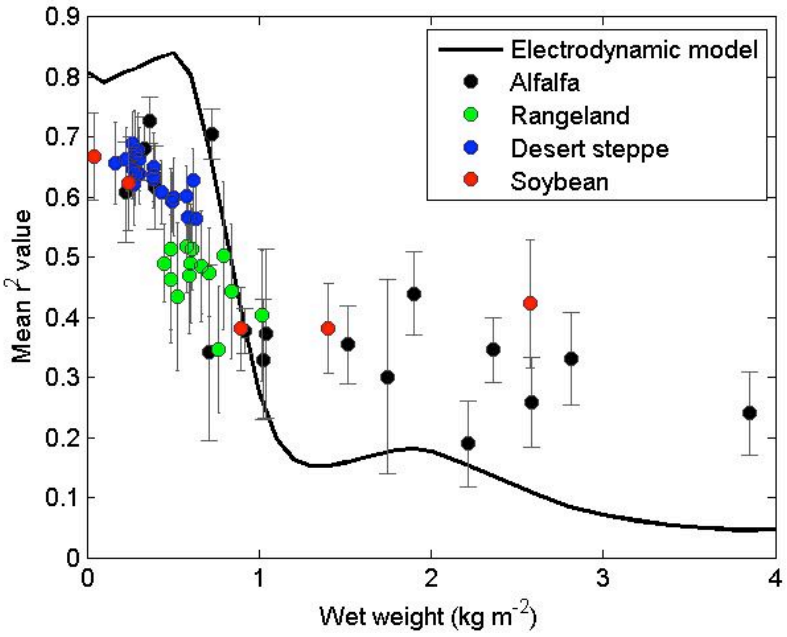

Figure 12: Average r^2 value for all sites for SNR curves from the electrodynamic model and the 'reconstructed' curve using (1) (black line). Dots indicate mean results +/- one standard deviation calculated using observed data from field sampling days for all available satellite tracks.

Table 1: Vegetation parameters for the four sites. Measured parameters were taken from field data. Antenna height is reported using the mean reflector height during low vegetation time periods for several satellites. The reported standard deviation is not used in this study but illustrates the extent of variation. Field data showed, for some sites, a wide range of % water contents. However, we used the reported mean % water content in permittivity estimation. Estimated parameters were assumed to vary directly with measured parameters. Calculated parameters were the result of the permittivity model in [35]. For reference, the permittivity of air is 1.0, and the real permittivity of dry snow is approximately 1.48 [40].

Site	Antenna Height (m)	Veg Height (cm)	Wet weight (kg m-2)	Biomass (kg m-2)	Range % water	Mean % water	Density (kg m-3)	Permittivity
	Measured						Estimated	Calculated
Soybean	2.96 +/- 0.09	0-105	0-4	0-1.1	67-83	72.5	725	1.050+0.012i
Alfalfa	2.69 +/- 0.15	0-80	0-5	0-0.9	59-89	74	740	1.080 + 0.019i
Rangeland	2.72 +/- 0.06	0-61	0-1.6	0-1.22	4-55	24	240	1.030+0.012i
Desert steppe	1.96 +/- 0.03	0-32	0-0.7	0-0.32	8-83	54	540	1.029+0.008i

Authors

Clara C. Chew received her B.A. in environmental studies from Dartmouth College in 2009. She is currently pursuing the Ph.D. in geological sciences at the University of Colorado, Boulder. Her research interests include surface hydrology and remote sensing.

Eric E. Small received a B.A. degree in geological sciences from Williams College in 1993 and the Ph.D. degree in earth sciences from

the University of California at Santa Cruz in 1998. He is a professor in the Department of Geological Sciences, University of Colorado, Boulder. His research is focused on land surface hydrology.

Kristine M. Larson received the B.A. degree in engineering sciences from Harvard University, Cambridge, MA, in 1985, and the Ph.D. degree in geophysics from the Scripps Institution of Oceanography, University of California at San Diego, La Jolla, in 1990. She was a member of the technical staff at JPL from 1988–1990. Since 1990, she has been a professor in the Department of Aerospace Engineering Sciences, University of Colorado, Boulder. Her research interests are focused on developing new applications and techniques for GPS.

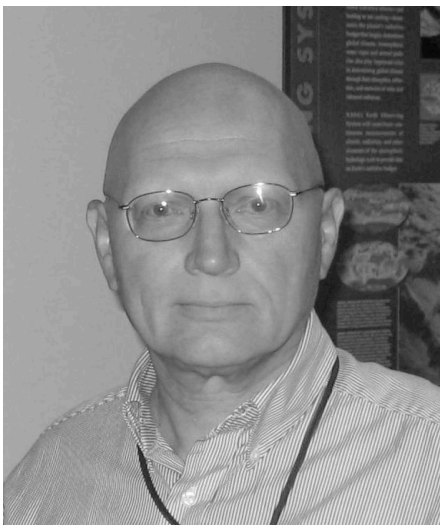

Valery U. Zavorotny (M'01–SM'03-F'10) received the M.Sc. degree in radio physics from Gorky State University, Gorky, Russia, in 1971, and the Ph.D. degree in physics and mathematics from the Institute of Atmospheric Physics, USSR Academy of Sciences, Moscow, in 1979. From 1971 to 1990, he was a Research Scientist with the Institute of Atmospheric Physics of the USSR Academy of Sciences, Moscow. In 1990, he joined Lebedev Physical Institute, Moscow, Russia. In 1991–2000, he was a CIRES Research Associate in the Environmental Technology Laboratory of the National Oceanic and Atmospheric Administration (NOAA), Boulder, CO, and became a NOAA/ETL physicist in 2000. His research interests include theory of wave propagation through random media, wave scattering from rough surfaces, and ocean and land remote sensing applications. Dr. Zavorotny is a member of URSI (Commission F) and the American Geophysical Union.